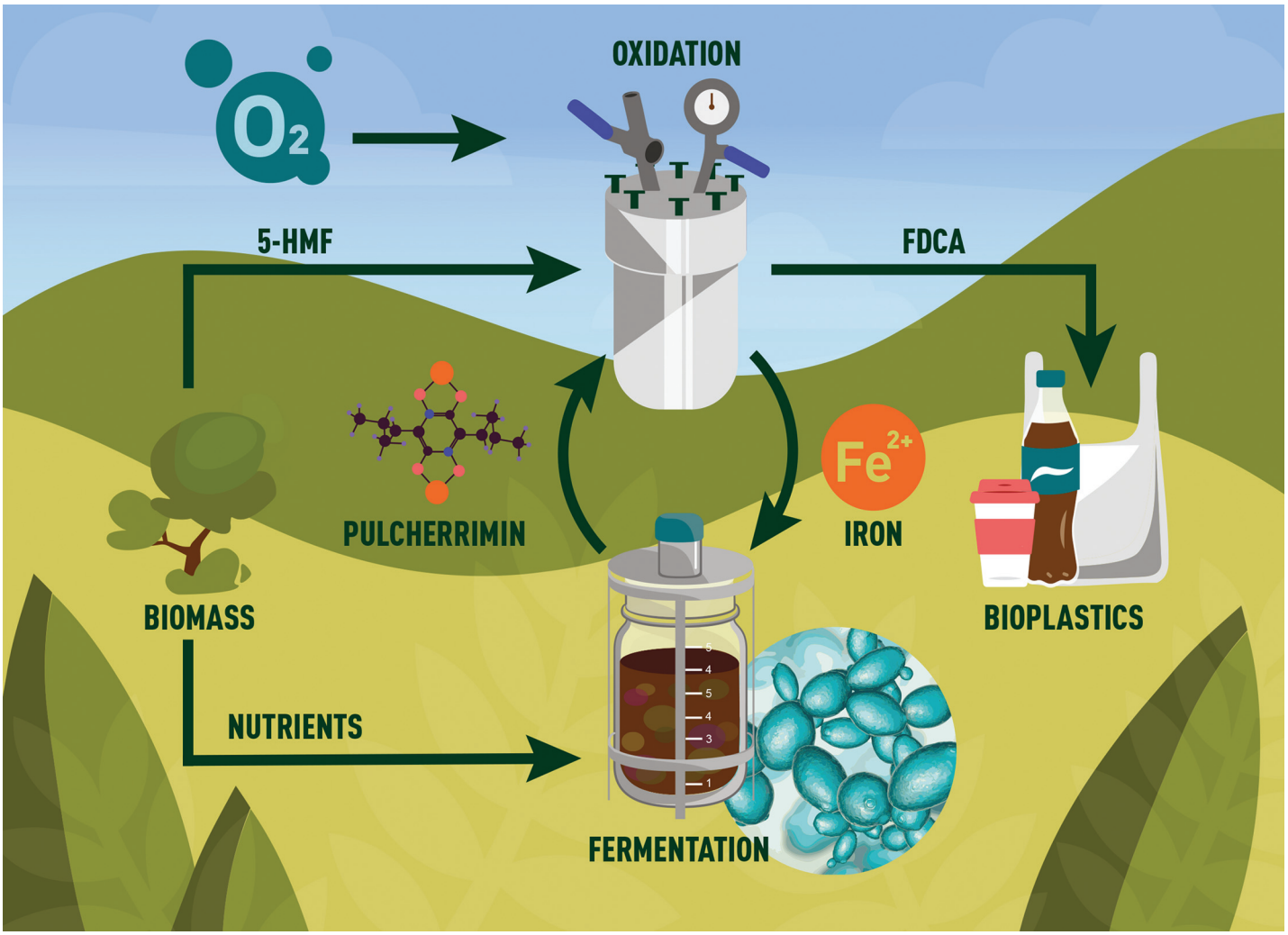

Showcasing research by Dr Jonathan Wagner, Dr Swathi Mukundan and Professor Sandra Dann *et al.* from Loughborough University, UK, and independent researcher Dr Fabio Santomauro, Spain.

Pulcherrimin: a bio-derived iron chelate catalyst for base-free oxidation of 5-hydroxymethylfurfural to furandicarboxylic acid

Pulcherrimin, a bio-mineral derived from yeast culture of Metchnikowia pulcherrima, was successfully applied to the selective base-free oxidation of 5-HMF into FDCA. The catalyst could be synthesised as part of a biorefinery approach and presents a commercially viable, environmentally friendly alternative to conventional noble metal catalysts.

Image reproduced by permission of Jonathan L. Wagner from *Green Chem.*, 2025, **27**, 4177.

As featured in:

See Jonathan L. Wagner *et al.*, *Green Chem.*, 2025, **27**, 4177.

Green Chemistry

PAPER

View Article Online
View Journal | View Issue

Cite this: *Green Chem.*, 2025, **27**, 4177

Pulcherrimin: a bio-derived iron chelate catalyst for base-free oxidation of 5-hydroxymethylfurfural to furandicarboxylic acid†

Swathi Mukundan, [a] Fabio Santomauro,[b] Daniel Miramontes Subillaga,[a] Noelia Villarroel,[a] Adriano Randi, [c,d] Sandra E. Dann, [c] Jose F. Marco [e] and Jonathan L. Wagner *[a]

Received 5th November 2024,
Accepted 27th February 2025

DOI: 10.1039/d4gc05641h

rsc.li/greenchem

This study explores the green and sustainable catalytic properties of pulcherrimin, a naturally occurring iron chelate, for the base-free oxidation of 5-hydroxymethylfurfural (5-HMF) to high-value products such as 2,5-furandicarboxylic acid (FDCA), a vital precursor for renewable bioplastics. Pulcherrimin, derived from *Metschnikowia pulcherrima*, selectively oxidised 5-HMF to 5,5-diformylfuran (DFF) at 100 °C, while at 120 °C, the oxidation proceeded efficiently to FDCA with a conversion of 73.3 ± 1.1%, and FDCA selectivity of 89.0 ± 1.9% under mild, base-free conditions. Adding a mild base enhanced overall conversion but diverted the reaction pathway towards 5-hydroxymethyl-2-furancarboxylic acid (HMFCA), reducing the FDCA yield. The reusability of the pulcherrimin catalyst was tested over five reaction cycles, retaining a conversion activity of 59.1% and FDCA selectivity of 39.8%. These findings establish pulcherrimin as a promising, water-tolerant biocatalyst with potential environmental advantages, such as base-free operation and simplified product recovery, contributing to greener catalytic processes. Eliminating a homogenous base co-catalyst makes the process greener by avoiding the need for subsequent neutralisation steps while reducing environmental and economic costs.

Green foundation

1. This work presents pulcherrimin, a bio-derived iron chelate, as a sustainable catalyst for the oxidation of 5-hydroxymethylfurfural (5-HMF) to 2,5-furandicarboxylic acid (FDCA) under mild, base-free conditions. The study demonstrates an efficient, and environmentally friendly pathway for FDCA production, avoiding the need for noble metal catalysts and homogeneous base co-catalysts.
2. The production of FDCA is critical for bioplastic synthesis, particularly in replacing petrochemical-based terephthalic acid in polyester manufacturing.
3. This study paves the way for biocatalyst-driven green chemistry, encouraging further exploration of bio-mineralised materials in catalysis. Future research will focus on enhancing catalyst stability and integrating bio-based catalysts into closed-loop biorefinery processes for scalable, low-impact chemical production.

1. Introduction

As the only natural source of renewable organic carbon, biomass will play a critical role in phasing out fossil resources as feedstock for sustainable chemical production. The global chemical market is seeing a growing presence of biomass-derived chemicals, expected to account for 22% of the market by 2025.[1] Unlike fossil fuels, which primarily contain carbon and hydrogen, biomass is rich in oxygen and other heteroatoms. This unique composition requires distinct chemical processes to effectively transform biomass into functional products.[2] Rather than simply replicating existing processes, the transition towards bio-based chemicals offers significant opportunities for new types of chemistries to yield products with improved properties and reduced impact, such as ecotoxicity and environmental persistence.[3,4]

One of the most important bio-based platform chemicals is 5-hydroxymethylfurfural (5-HMF), which can be produced through the dehydration of cellulose-derived glucose, includ-

[a]*Department of Chemical Engineering, Loughborough University, Loughborough, LE11 3TU, UK. E-mail: J.L.Wagner@lboro.ac.uk*
[b]*Independent researcher, Carrer Sant Vicent 34, 46138 Rafelbunyol, Valencia, Spain. E-mail: fabiotecno@yahoo.it*
[c]*Department of Chemistry, School of Science, Loughborough University, Loughborough LE11 3TU, UK*
[d]*R3V Tech Ltd, Luinc. Holywell building, Holywell way, Loughborough, LE11 3UZ, UK*
[e]*Instituto de Química Física Blas Cabrera, CSIC, Serrano, 119, 28006 Madrid, Spain*
† Electronic supplementary information (ESI) available. See DOI: https://doi.org/10.1039/d4gc05641h

ing from agricultural and forestry residues (*e.g.*, corn stover, wheat straw, sawdust and wood chips), and energy crops such as miscanthus.[5–7] Stepwise oxidation of 5-HMF *via* 2,5-diformylfuran (DFF) or 5-hydroxymethyl-2-furancarboxylic acid (HMFCA) yields 2,5-furandicarboxylic acid (FDCA), which can substitute benzene-1,4-dicarboxylic acid (terephthalic acid, TA) in the production of polyesters and other polymers.[8] Replacing conventional polyethylene terephthalate (PET), one of the most commonly used plastic packaging materials, with FDCA-based polyethylene furanoate (PEF) could reduce its cradle-to-grave greenhouse gas emissions by 45–55%, with potential global CO_2 savings of 20–35 MT per year, based on current PET use.[9] As the bioplastics market is projected to increase from USD 9.2 billion in 2023 to USD 20 billion by 2026,[10,11] there is significant demand for scaling up FDCA production. Moreover, the partial oxidation intermediate DFF in itself is a valuable chemical precursor with applications ranging from biopolymer synthesis and biobased polyurethane thermosets to fluorescent materials and therapeutics.[12]

However, the commercial use of 5-HMF derived FDCA is currently limited by its high manufacturing costs compared to TA production.[13] Therefore, there is a high industry demand for more cost-effective production methods of FDCA. This could be achieved through novel synthetic approaches, such as the dehydration of galactaric acid (mucic acid), a dicarboxylic sugar acid derived from galactose or lactose, under mild conditions.[14] Recent studies have demonstrated the efficient use of metal-based catalysts, such as sulfuric acid combined with boric acid, to dehydrate galactaric acid to FDCA with high selectivity.[15] Furthermore, esters of FDCA can be produced *via* direct esterification during the dehydration process, facilitating the preparation of monomers for polymer applications. These processes circumvent intermediate oxidation steps (*e.g.*, DFF or FFCA) and align with sustainable chemistry principles by utilising renewable sugar-based feedstocks. However, the scalability of this approach is limited by the availability and cost of galactaric acid and associated challenges in large-scale production.

In contrast, the oxidation of 5-HMF remains a more established and economically viable route. The oxidation of 5-HMF into FDCA can be catalysed by noble metal catalysts (Au, Pt, Pd, Ru), but their high cost and environmental impact make them economically unattractive.[16] Transition metal catalysts (Fe, Cu, V, *etc.*) are cheaper alternatives. Still, their lower activities impose longer reaction times and require the addition of homogeneous base co-catalysts, such as NaOH or KOH, to accelerate the oxidation process. While base catalysts facilitate the deprotonation of intermediates to promote the formation of FDCA,[17] their use imposes additional neutralisation and purification steps and results in the formation of salts and other byproducts that increase the environmental footprint of the process.[18] Moreover, using base catalysts can corrode the reactor vessel and contaminate the other catalysts used for the reaction. Therefore, base-free oxidation methods are considered greener and more sustainable. Another challenge is the poor stability of many commonly used supports for both noble and transition metal catalysts (*e.g.*, silica, alumina) under hydrothermal conditions. This requires the substitution of water with organic reaction solvents such as DMF or DMSO, incurring significant costs and adverse environmental effects linked to their recovery and disposal.[19]

Enzymatic oxidation with laccase, alcohol oxidase, or aryl-alcohol oxidase has been evaluated as a promising alternative for 5-HMF conversion to FDCA.[20] For instance, alcohol oxidase from *Pichia pastoris* can efficiently convert 5-HMF to DFF and then to FDCA in the presence of flavin adenine dinucleotide.[21] This enzyme works through a series of intermediates but requires careful control of reaction conditions to prevent the accumulation of inhibitory byproducts like hydrogen peroxide.[21] Aryl-alcohol oxidase (AAO) from the fungus *Pleurotus eryngii* is another enzyme catalyses the oxidation of 5-HMF to FDCA. However, its effectiveness is often limited by the slow oxidation of intermediates, such as the conversion of 5-formyl-2-furancarboxylic acid (FFCA) to FDCA.[22] The use of enzymatic catalysts is limited by issues of stability, reusability, and scalability, as well as by low reaction rates.[23]

Another potential alternative catalyst for 5-HMF oxidation is the bio-mineral pulcherrimin, a natural iron chelate produced by some yeasts (*Metschnikowia*, *Lipomyces*, *Kluyveromyces*, *etc.*) and bacteria (*Bacillus and Streptomyces*).[24] The molecular structure of pulcherrimin, a ferric salt of pulcherriminic acid (3,6-dihydroxy-2,5-diisobutylpyrazine-1,4-dioxide), was initially proposed by Kluyver,[24] and later supported by Cook and Slater.[25] Pulcherrimin can be easily recovered from the culture medium following fermentation, at concentrations of up to 240 mg L^{-1} (wild strain of *M. pulcherrima*) and 556 mg L^{-1} (genetically engineered strain of *B. licheniformis*).[26] Research into *M. pulcherrima* has focused on its role in post-harvest protection of fruits and vegetables, wine biotechnology and, more recently, single-cell oil production, where iron availability might play a significant role in the modulation of microbial population dynamics.[27,28] Combining pulcherrimin production with the synthesis of other high-value biocompounds could offset production costs. For example, *M. pulcherrima* can accumulate high amounts of food-grade single-cell oil (>40% w/w) and produce 2-phenylethanol (up to 1500 mg L^{-1}), while *Bacillus licheniformis* is commercially used to produce the enzyme subtilisin, and as a probiotic in animal feed, with potential to produce the biofuel 2,3-butandiol.[29,30]

Chemically, pulcherrimin is an iron chelate of pulcherriminic acid that self-organises into a hydrophilic metal–organic complex through an enzyme-free process. Pulcherrimin has an iron content of around 12.7%, is insoluble in organic solvents and only slightly soluble in water. It is stable at temperatures of up to 120 °C and displays excellent resistance to extreme acidic conditions, while promptly dissolving in concentrated alkali.[24] This complex structure, characterised by four oxygen atoms from pulcherriminic acid coordinating with two iron atoms, may help modulate iron reactivity to mimic the electron configurations of more expensive metal catalysts, such as platinum or ruthenium, making it a cost-effective option for industrial catalytic applications. Being produced through microbial

fermentation process, easily purified and recovered from water and organic solvents, makes pulcherrimin an attractive candidate for catalytic studies.

The hypothesis of the current study is that pulcherrimin, a metal–organic complex, possesses significant unexplored oxidative properties suitable for catalytic applications. This study aims to investigate the catalytic properties of pulcherrimin by first characterising its physical and chemical properties, followed by testing its catalytic activity for the oxidation of 5-HMF to FDCA. The performance of pulcherrimin is compared to a traditional α-Fe_2O_3 catalyst supported on carbon with the same iron content. Furthermore, the reusability of pulcherrimin for the catalytic oxidation of 5-HMF was assessed. To our knowledge, this is the first time pulcherrimin has been explored for catalytic applications, marking a novel use of a naturally occurring metal–organic complex for 5-HMF oxidation. The insights gained contribute to the development of environmentally friendly catalytic systems and could have broad implications for catalyst design in the bio-refining industry.

2. Experimental section

2.1. Materials

Yeast extract, D-(+)-glucose, anhydrous (99%), iron(III) nitrate nonahydrate (99+ %), D-mannitol (98+ %), L(+)-tartaric acid, L(−)-malic acid (99%), sodium carbonate, NaOH, sodium citrate dihydrate were all purchased from Fisher scientific. Peptone Hy-Soy® T, D-(−)-fructose, ammonium phosphate dibasic, iron(III) chloride (97%), ammonium sulfate (≥99%), potassium phosphate dibasic (≥98%), cobalt(II) chloride hexahydrate, ammonium molybdate tetrahydrate (81.0–83.0% MoO_3 basis), iron(II) sulfate heptahydrate (≥99%), magnesium sulfate anhydrous (≥99.5%), calcium chloride dihydrate (≥99%) were all purchased from Merck. Active culture of *Metschnikowia pulcherrima* (NCYC 373) was purchased from the National Collection of Yeast Cultures (NCYC), Norwich, U.K. Furan-2,5-dicarboxylic acid (98%) and 5-(hydroxymethyl)furfural (98%) were purchased from Thermo Scientific, U.K. 2,5-Furandicarboxaldehyde (97%) was purchased from scientific laboratory supplies. Activated charcoal (DARCO, 100 mesh particle size) and Yeast Peptone Dextrose (YPD) broth were sourced from Sigma Aldrich. Agar was purchased from Millipore.

2.2. Synthesis of pulcherrimin and Fe_2O_3/C (baseline catalyst)

Metschnikowia pulcherrima (strain NYC 373) was grown on YPD agar plates at 20 °C (Fig. 1a). A colony was picked up to inoculate a 100 mL YPD medium (10 g L^{-1} yeast extract, 20 g L^{-1} peptone, 20 g L^{-1} glucose) under sterile conditions and incubated at 20 °C on a shaker at 180 rpm. After 24 h, 20 mL of the culture was used as inoculum and added to 2 L of non-sterile synthetic grape juice media (SGM) in a 5L bioreactor (Fig. 1b) at 110 rpm with an aeration of 20 L min^{-1}. The SGM, a modified version of the recipe reported by Bejaoui *et al.*,[28,31] consisted of 70 g L^{-1} glucose, 30 g L^{-1} fructose, 7 g L^{-1} tartaric acid, 10 g L^{-1} malic acid, 2 g L^{-1} $(NH_4)_2HPO_4$, 0.67 g L^{-1} KH_2PO_4, 1.5 g L^{-1} $MgSO_4{\cdot}7H_2O$, 0.15 g L^{-1} NaCl, 0.15 g L^{-1} $CaCl_2$, 0.15 g L^{-1} $FeSO_4{\cdot}7H_2O$, 0.0075 g L^{-1} $ZnSO_4{\cdot}7H_2O$ with the pH adjusted to 4 before inoculation. The culture was incubated in the bioreactor for 7–10 days at a temperature of 20 ± 5 °C.

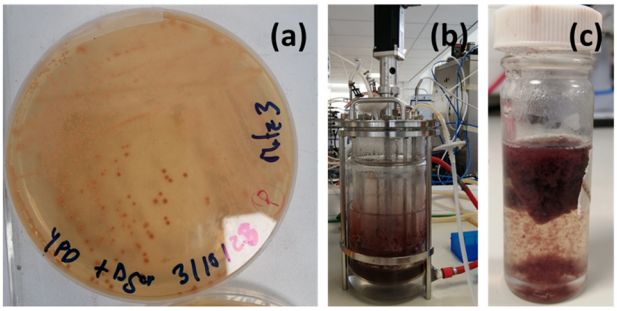

Fig. 1 (a) YPD agar plates for *Metschnikowia pulcherrima* (strain NYC 373) (b) *Metschnikowia pulcherrima* grown in sterile synthetic grape juice media (SGM) in a 5L bioreactor. (c) Pulcherrimin precipitated after incubation at 85 °C for 1 h.

The culture was centrifuged at 4 °C at 4700 rpm for 15 min, resulting in a solid pellet (a compact layer of cells at the bottom) with the supernatant liquid above it. The supernatant was decanted off, and the pellet was then resuspended in methanol at 4 °C (50 mL per 10 g of wet yeast biomass). After overnight treatment, the cells were centrifuged again at 4700 rpm, 4 °C for 15 min, followed by two washes with distilled water. The resulting pellet was resuspended in 2 M NaOH and centrifuged (4 °C, 4700 rpm, 15 min). The supernatant was collected, and the pH adjusted to 1.0 with 4 M HCl before incubating at 85 °C for 1 h. The precipitated pigment was then collected by centrifugation at 4700 rpm, 4 °C for 30 min and washed three times with distilled water (Fig. 1c). Finally, the pigment was dried at 60 °C for 18 h.

The iron oxide catalyst supported on activated carbon (α-Fe_2O_3/C) was prepared using a simple wetness impregnation method, achieving a metal content of 11.6 wt%. This method was adopted as described in previous literature.[32] Initially, the activated carbon was dried at 70 °C overnight in an oven. Subsequently, a measured amount of the aqueous iron precursor solution was mixed with the activated carbon and stirred for 8 h at ambient temperature. The mixture was then subjected to water removal through a rotary evaporator at 50 °C, followed by drying overnight at 100 °C. Finally, the material was heat treated at 550 °C for 8 h, with a nitrogen flow of 30 mL min^{-1} in a tube furnace.

2.3. Pulcherrimin characterisation

The formation of pulcherrimin was confirmed using a PerkinElmer Lambda 35 UV/VIS spectrometer at a wavelength of 410 nm. Raman analysis was performed with a Horiba Jobin Yvon HR LabRAM confocal Raman microscope in backscatter-

ing configuration, using a red argon laser operating at 633 nm filtered to 10% power. Fourier Transform-Infrared Spectroscopy (FT-IR) was conducted using a PerkinElmer Spectrum 100, recording data between 4000–250 cm^{-1} using potassium bromide (KBr) pellets. Elemental composition analysis (CHN) was conducted using a Thermo Fisher Scientific Flash SMART elemental analyser at the Grant Institute, University of Edinburgh, with furnace temperatures set to 950 °C. Inductively coupled plasma atomic emission spectroscopy (ICP-AES) was performed using an Agilent MP system, with samples digested in 5 mL aqua regia in a microwave reaction system at 220 °C for 40 min, then filtered through a 0.45 μm PTFE syringe filter. Nitrogen adsorption–desorption measurements were conducted at −196 °C using a Micromeritics TriStar II 3020 surface area and porosity analyser, with samples degassed under vacuum at 100 °C for 6 h. The Brunauer–Emmett–Teller (BET) method was used to calculate specific surface area, and pore volume was determined from nitrogen adsorbed at a relative pressure (P/P_0) of 0.99. Thermogravimetric analysis (TGA) was performed with a Star system TGA/DSC 1, heating samples to 800 °C at 5 °C min^{-1} in an airflow of 40 mL min^{-1}. Scanning electron microscopy (SEM) was conducted using a JEOL JSM 7100F FEGSEM instrument at 5 kV. Mössbauer data were collected at 298.0 K and 8 K using a standard constant acceleration spectrometer with a ^{57}Co (Rh) source, with velocity scales calibrated using a 6 μm thick α-Fe foil. The chemical isomer shifts were referred to the centroid of the spectrum of α-Fe at room temperature.

2.4. Catalytic oxidation reaction

The oxidation of 5-HMF was conducted in a 100 mL compact high-pressure Parr reactor (Model 5513). Typically, 40 mL of a 4.15 mmol aqueous solution of 5-HMF (0.52 g) was placed in the reactor vessel. Pulcherrimin (0.05 g) was added, resulting in an approximate weight ratio of 10 : 1 (HMF to pulcherrimin). The reactor was then heated to a preset reaction temperature (100 °C, 120 °C, or 140 °C) at a rate of approx. 5 °C min^{-1}. For reactions with added base, 0.008 M NaOH was included. The reaction was assumed to have started once the set temperature was reached. Samples of 0.4 mL were withdrawn hourly using a sampling port, centrifuged, and the liquid sample was analysed by GC-MS. The reaction was conducted for 10 h, after which the reactor was cooled to ambient temperature. Pulcherrimin was separated by filtration using pre-dried and weighed Whatman filter paper (grade 1), dried overnight at 80 °C, and weighed to determine the amount recovered.

The % conversion of 5-HMF, the % selectivity and % yield of products were calculated using the following formulae:

$$\%\ \text{conversion of HMF} = \left(1 - \frac{\text{number of moles of HMF in product}}{\text{number of moles of HMF in feed}}\right) \times 100 \quad (1)$$

$$\%\ \text{yield of product} = \left(1 - \frac{\text{number of moles of product formed}}{\text{number of moles of HMF in feed}}\right) \times 100 \quad (2)$$

$$\%\ \text{selectivity of product} = \left(1 - \frac{\text{yield of product}}{\%\ \text{conversion of 5-HMF}}\right) \times 100 \quad (3)$$

2.5. Catalyst reusability tests

Reusability tests were conducted with recovered pulcherrimin after drying at 80 °C. To account for catalyst losses (8–14%), fresh catalyst was added for repeatability studies, following the same procedure as described in section 2.4. Catalyst recovery was calculated as:

$$\%\ \text{catalyst recovery} = \frac{\text{catalyst used for reaction (g)} - \text{catalyst recovered (g)}}{\text{catalyst used for reaction (g)}} \times 100 \quad (4)$$

The reusability test reaction yields were adjusted to exclude the contribution of the fresh catalyst using the following equation:[29]

$$Y_{\text{corrected}} = Y_{\text{actual}} - \frac{m_{\text{FC}}}{m_{\text{TC}}} \times (Y_{\text{FC}} - Y_{\text{NC}}) \quad (5)$$

where Y is yield of different products, m_{FC} and m_{TC} are the weights of fresh and total catalyst, respectively, and Y_{FC} and Y_{NC} are the yields obtained from the initial catalytic and non-catalytic reactions, respectively.

2.6. Product analysis

The compounds were quantified using a gas chromatograph equipped with an Agilent HP GC systems 6890 series FID and a Resteck Stabilwax-MS capillary GC column (30 m length, 0.25 mm internal diameter, and 0.25 μm film thickness). The sample was diluted with methanol in the ratio 80 : 20 (methanol: sample) for analysis. The carrier gases used were compressed helium and compressed air, along with hydrogen gas supplied at 99.99% purity by an H13-600N-10 Mars hydrogen generator. The temperature program for the analysis began with an initial oven temperature of 60 °C held for 1 min, followed by a ramp to 260 °C at a rate of 10 °C min^{-1}, and held at 260 °C for 1 min. The injection port was maintained at 220 °C. The concentrations of 5-HMF, DFF, and FDCA in the reaction mixture were measured using the external calibration method. Calibration curves were prepared with pure compounds as standards. Since the concentrations of these compounds were within the solubility limit in water, they were dissolved in water at 30 °C for calibration purposes. The unknown compounds were identified using an Agilent 5975C GC-MS inert MSD equipped with a DB Wax column (30 m length, 0.25 mm internal diameter, and 0.25 μm film thickness). Helium served as the carrier gas. The injection temperature was set at 220 °C with a split ratio of 50 : 1. The column temperature was programmed to start at 50 °C and held for 5 min, then increased to 150 °C at a rate of 15 °C min^{-1} and held for 1 min, followed by a final increase to 250 °C at 5 °C min^{-1}, and held for 1 min.

3. Results and discussion

3.1. Pulcherrimin characterisation

Pulcherrimin was synthesised in triplicate and extracted exclusively from the cells despite being primarily an extracellular compound. A hydrolysis step was included during recovery to maximise yield, as some pulcherrimin or its precursors may remain cell-associated, bound to the cell surface, or embedded within the extracellular matrix.[33] The average yield across all batches was 0.2639 ± 0.0422 g g^{-1} of the dried harvested biomass (cultivated cells of *Metschnikowia pulcherrima*).

The C, H, and N composition of pulcherrimin was 47.8 ± 0.1%, 6.7 ± 0.3%, and 8.9 ± 0.6%, respectively, with an Fe content of 11.2 ± 0.2%, consistent with previously reported values.[24] The molecular formula of pulcherrimin is $C_{16}H_{18}N_2O_4Fe$, corresponding to a theoretical Fe content of 15.7% by mass. The formation of pulcherrimin was confirmed through UV-VIS analysis (Fig. 2a) by solubilising pulcherrimin in 2 M NaOH. The analysis revealed three characteristic absorption peaks at 240, 280, and 410 nm which are consistent with literature values, thereby confirming the formation of pulcherrimin.[26] The peak at 240 nm is associated with $\pi \rightarrow \pi^*$ transitions in conjugated systems, which could indicate the presence of double bonds and the aromatic structure of pulcherrimin, while the 280 nm peak corresponds to aromatic amino acids within pulcherrimin.[34] The absorption at 410 nm is generally linked to transition metal complexes involving d–d transitions, as observed in heme-containing proteins. This peak is indicative of highly conjugated organic dyes and pigments, where extended conjugation leads to absorption in the visible spectrum.[35]

To evaluate the thermal stability of pulcherrimin in an oxidative environment, thermogravimetric analysis (TGA) was conducted, revealing gradual decomposition starting at approximately 140 °C (Fig. 2b), consistent with values reported in the literature.[24] After heating to 800 °C, around 30% of the sample mass remained, which can be partially attributed to the formation of iron oxide in the combustion residue residues. For instance, using a pulcherrimin iron content of 11.2% as obtained by ICP analysis should theoretically yield approximately 16.0% Fe_2O_3. However, the observed discrepancy in the iron oxide yield may be due to residual impurities within the pulcherrimin structure, potentially leading to an iron content lower than expected. These impurities could include organic residues or other non-volatile components that remain within the complex, reducing the overall proportion of Fe_2O_3 formed. Based on this analysis, we selected 140 °C as the upper temperature limit for evaluating the catalytic activity of pulcherrimin. Pulcherrimin was tested for stability by heating it in water at 120 °C for 10 h, followed by filtration. Any solvent residue was evaporated and weighed. The results showed no residue and 0.4% mass loss, confirming the stability of pulcherrimin under the reaction conditions (results shown in ESI†).

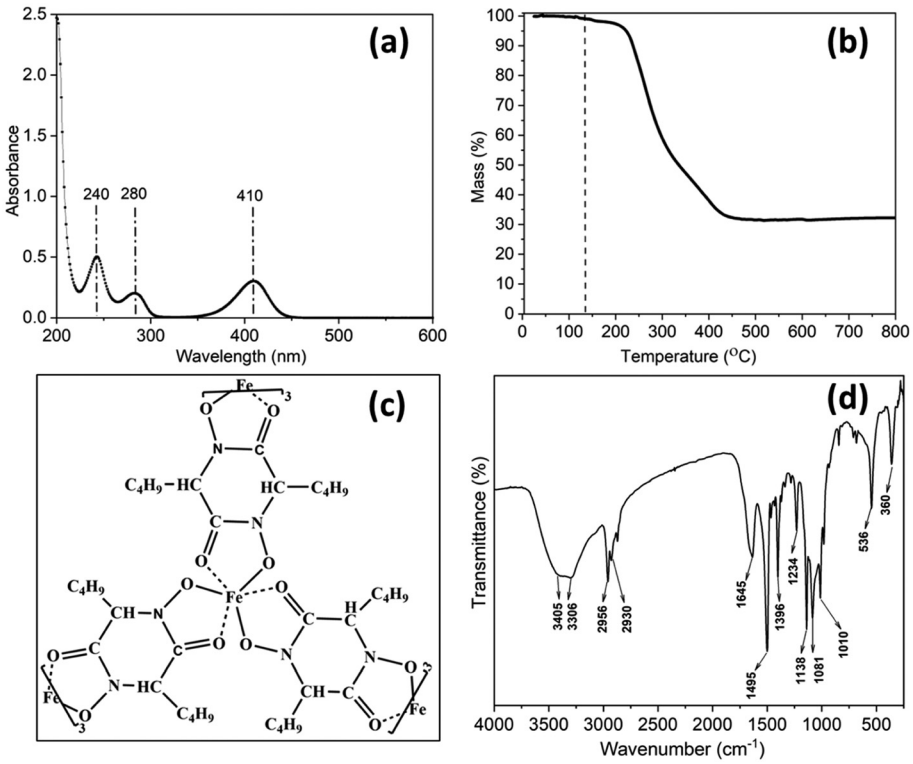

Fig. 2 (a) Ultra-violet absorption spectrum of pulcherrimin recorded at a wavelength of 200–600 nm, (b) TGA profile performed under air at 5 °C min^{-1}, (c) pucherrimin: unit configuration, based on the structure reported by Kluyver *et al.*,[24] (d) FT-IR of pulcherrimin.

As outlined by Kluyver *et al.*,[24] pulcherrimin comprises various functional groups as depicted in the molecular structure (Fig. 2c). To verify these functional groups, FT-IR spectroscopy was utilised, which provides insights into the functional groups by analysing the vibrational modes of the molecules. The FT-IR spectrum of the synthesised pulcherrimin (Fig. 2d) reveals the molecular composition through several distinct absorption bands. The presence of N–H stretching vibrations at 3405 cm^{-1} and 3306 cm^{-1} is consistent with primary amines, corresponding to the N–H bonds apparent in the pulcherrimin molecular structure.[36,37] Similarly, the observed C–H stretching vibrations at 2956 cm^{-1} and 2930 cm^{-1} align with the various methyl groups present in pulcherrimin. The band at 1645 cm^{-1} which corresponds to C=O stretching vibrations, confirms the ketonic linkages illustrated in the pulcherrmin complex.[38] Notably, the peak at 1495 cm^{-1} is indicative of N–O stretching. The detection of C–H bending at 1396 cm^{-1} and C–N stretching at 1234 cm^{-1} further confirms the aliphatic rings and nitrogen connections within the structure. The series of C–O stretching vibrations at 1138 cm^{-1}, 1081 cm^{-1}, and 1010 cm^{-1}, are indicative of various ether or ester linkages as expected in pulcherrimin. Importantly, the significant peak at 536 cm^{-1} attributed to Fe–O stretching vibrations confirms the incorporation of iron within the pulcherrimin matrix, validating the iron-oxygen bonds that are vital to the metal–organic structure of pulcherrimin.[39] The FT-IR spectrum obtained closely aligns with that reported by MacDonald,[40] thus confirming the presence of key functional groups and the structure of pulcherrimin. The presence of minor unaccounted peaks may indicate impurities. Further investigation to determine their origins and potential effects on the compound's properties is beyond the scope of the current work.

Zdaniauskienė and coworkers,[41] recorded surface-enhanced Raman Spectroscopy (SERS) on pulcherrimin. Intense sharp bands from the C=C stretching vibrations for the pyrazine ring should be observed at approximately 1600 cm^{-1}, with asymmetric stretching vibrations of CNC at around 1410 cm^{-1}. Scissoring vibrations of the CH_2 groups, coupled with the deformation motion of CH_3, should then appear at roughly 1440 cm^{-1}. However, these bands are all obscured by the characteristic and broad D and G bands of disordered graphite at 1350, and 1580 cm^{-1} as observed in Fig. 3a, indicating that the fragile pulcherrimin has decomposed in the instrument.

Mössbauer spectroscopy was performed to understand the oxidation state and coordination geometry of iron in pulcherrimin. The spectrum recorded at room temperature only showed a paramagnetic doublet with isomer shift δ = 0.41 mm s^{-1} and quadrupole splitting Δ = 0.66 mm s^{-1} (Fig. 3b). These hyperfine parameters are characteristic of an octahedrally-coordinated high spin, $S = 5/2$, Fe^{3+} species as is expected for pulcherrimin. Data recorded at 8K (not shown) indicated that the quadrupole splitting is temperature independent, thus confirming the high spin nature of the Fe^{3+} species. The low-temperature spectra did not show any magnetically ordered species at all, ruling out the possible presence of superparamagnetic (nanosized) iron oxide species that may have gone undetected by other techniques, which clarifies the absence of impurities in the sample. The use of Mössbauer spectroscopy for characterising pulcherrimin appears to be scarce, with only one previous study reporting its Mössbauer spectra (both at RT and low temperatures).[42] The results reported by Mažeika *et al.* are consistent with those presented here: (i) the Mössbauer spectrum at room temperature shows a single paramagnetic doublet characteristic of a high spin Fe^{3+} species, (ii) the quadrupole splitting is temperature independent.[42] However, the Δ value reported by Mažeika *et al.* (0.85 mm s^{-1}) is larger than the value measured presently (0.66 mm s^{-1}). Since for a $S = 5/2$ Fe^{3+} species the quadrupole splitting value depends only on the charges surrounding the iron ion (lattice contribution), the data suggest that the Fe^{3+} pulcherrimin species studied by Mažeika *et al.* had a more distorted octahedral geometry than the one reported here.

3.2. 5-HMF oxidation reactions

3.2.1. Baseline reactions with Fe_2O_3/C catalyst. Initial experiments at 120 °C without a catalyst showed negligible conversion of 5-HMF after 10 h, indicating that oxygen alone is insufficient to drive the reaction.[43] Subsequently, the performance of a 11.6 ± 0.4% Fe/C baseline catalyst (primarily in the form of Fe_2O_3), was tested for the oxidation of 5-HMF under both non-basic and basic conditions (Fig. 4). This catalyst was

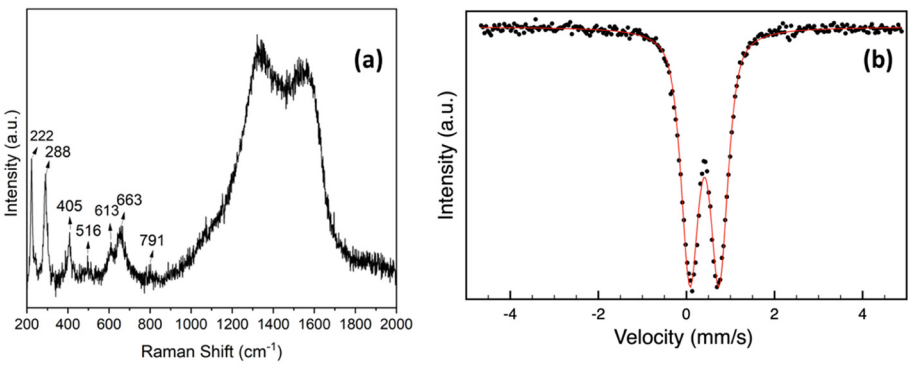

Fig. 3 (a) Raman spectra, (b) Mössbauer spectra of pulcherrimin.

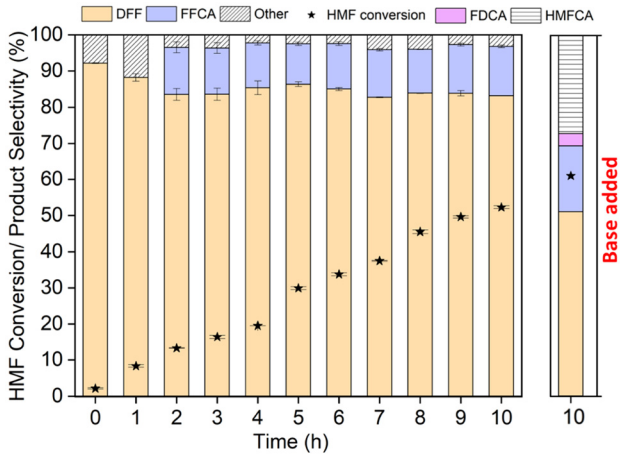

Fig. 4 5-HMF conversion and product selectivity with respect to time over Fe_2O_3/C catalyst, with and without the addition of a base (0.008 M NaOH) (Reaction conditions: 40 mL of 4.15 mmol 5-HMF, 0.05 g of catalyst, 120 °C, 10 bar O_2 gas).

designed to match the Fe content as pulcherrimin, allowing for a direct comparison of catalytic activities between Fe_2O_3/C and pulcherrimin. All experiments were conducted in duplicate over 10 h, with 0.2 mL samples withdrawn every hour to monitor the catalyst activity over time. The HMF conversion at 120 °C was found to increase linearly over time, from 8.4 ± 0.3% after 1 h to 52.4 ± 0.4% after 10 h. After one hour, DFF was the only identifiable reaction product with a selectivity of 88.2 ± 1.0%. DFF is produced by the selective oxidation of the hydroxymethyl group in HMF instead of the more reactive α,β-unsaturated aldehyde group.[44] After 2 h, FFCA (5-formyl-2-furancarboxylic acid) was detected as secondary reaction product, formed by the oxidation of one of the aldehyde groups in DFF into a carboxyl group (–COOH). Within the following 8 h, the selectivity towards DFF (83.2%) and FFCA (13.3–13.8%) remained approximately constant, while 5-HMF conversion continued to increase.

The primary objective of this study is the synthesis of FDCA. The oxidation of DFF to FDCA involves FFCA as a key intermediate. Specifically, the oxidation of a single aldehyde group in DFF to a carboxyl group (–COOH) yields FFCA, while the subsequent oxidation of the second aldehyde group results in the formation of FDCA. The product distribution observed indicates that under studied conditions, the Fe_2O_3/C catalyst predominantly facilitates partial oxidation of 5-HMF into DFF and FFCA but is unable to catalyse the subsequent oxidation of the second aldehyde group to form the desired FDCA product. This is consistent with previous studies that identified the conversion of FFCA to FDCA as the rate-limiting step in the overall oxidation process, primarily due to the relatively low reactivity of FFCA compared to other intermediates.[45,46] This reduced reactivity necessitates more severe reaction conditions or the use of more active noble-metal catalysts to achieve efficient and high-yield conversion to FDCA. For instance, Walton *et al.*, reported the use of TEMPO (2,2,6,6-Tetramethylpiperidine 1-oxyl) as a co-catalyst with MIL-100(Fe) metal–organic framework (MOF) to facilitate the full conversion of FFCA to FDCA during HMF oxidation.[46] TEMPO works by efficiently abstracting hydrogen atoms from the aldehyde group of FFCA, forming an oxoammonium ion. This ion then facilitates the transfer of electrons, promoting the further oxidation of the aldehyde to the carboxylic acid group, thereby converting FFCA into FDCA.

Effect of addition of base (NaOH). To test the impact of adding base, a single 10 h experiment run was conducted with the addition of 0.008 M NaOH. Following the addition of the base, the conversion of HMF increased to 61.2% after 10 h, compared to 52.4% under non-basic conditions. The presence of base also facilitated the formation of FDCA within the product streams, as expected. In terms of product selectivity at the end of 10 h, 51.1% DFF, 18.3% FFCA, and 3.4% FDCA were formed, along with the formation of 27.2% HMFCA (5-Hydroxymethyl-2-furancarboxylic acid). It has been reported in the literature, when the reaction occurs in a basic aqueous solution, it advances through the oxidation of the aldehyde group, with the oxidation of the alcohol functionality acting as the rate-limiting step.[47] Therefore, HMFCA, as a partially oxidised product, serves as an intermediate in the oxidation pathway from HMF to FDCA in aqueous basic conditions.

In the reaction over Fe_2O_3/C without base, the formation of FDCA proceeds *via* the DFF pathway. In this route, the hydroxymethyl group (–CH_2OH) at the 5-position of HMF is selectively oxidised to an aldehyde group (–CHO), forming DFF, which is then further oxidised to FDCA. This pathway is commonly observed with supported noble metal catalysts (*e.g.*, Pt, Au, Pd) and strong oxidants, which provide active sites facilitating both oxidation steps. However, when a base is introduced, the reaction suggests an alternative pathway, where the aldehyde group (–CHO) at the 2-position of HMF is selectively oxidised to a carboxylic acid group (–COOH), forming HMFCA. The base appears to activate this pathway by promoting selective oxidation, contrasting with the degradation of DFF often observed under alkaline aqueous conditions, where side reactions like humin formation occur. These results suggest that Fe_2O_3/C effectively catalyses partial oxidation of HMF to DFF and FFCA, especially under non-alkaline aqueous conditions. The introduction of NaOH led to only a minor increase in overall conversion while also producing a range of undesirable side products, such as HMFCA and other furan derivatives, indicating that the base had limited beneficial effects on the overall reaction efficiency.

3.2.2. 5-HMF oxidation with pulcherrimin. The catalytic performance of pulcherrimin for the oxidation of 5-HMF is illustrated in Fig. 5. The reaction was conducted at the same conditions as the Fe_2O_3/C without the addition of an alkaline base. The reaction conducted at 120 °C (Fig. 5b) showed that HMF conversion reached 14.3 ± 0.4% after 1 h, increasing to 73.3 ± 1.1% after 10 h, significantly exceeding HMF conversion over Fe_2O_3/C (52.4%). DFF was formed as the primary oxidation product, with high initial selectivity of 87.6 ± 1.9% after 1 h. However, unlike the Fe_2O_3/C-catalysts reactions, as reac-

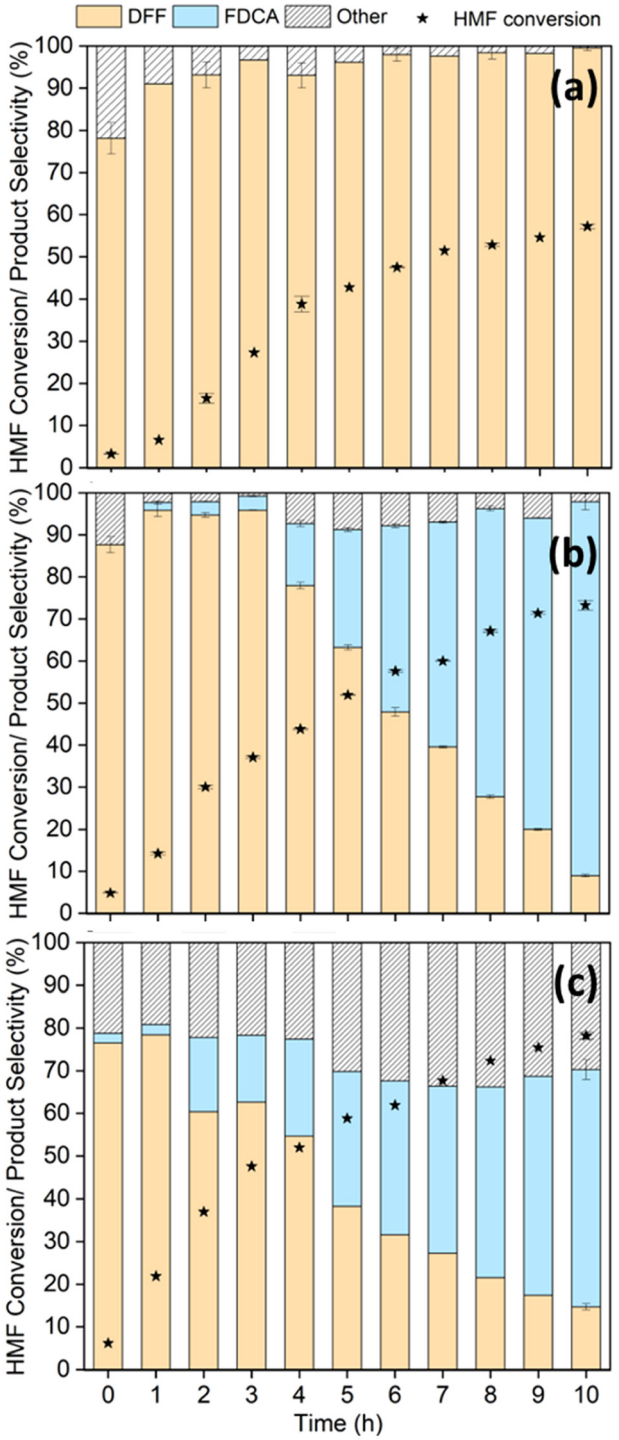

Fig. 5 5-HMF conversion and product selectivity with respect to time over pulcherrimin catalyst at (a) 100 °C, (b) 120 °C, (c) 140 °C (Reaction conditions: 40 mL of 4.15 mmol 5-HMF, 0.05 g of catalyst, 10 bar O_2 gas).

tion time is increased, DFF is directly converted into FDCA, while the intermediate FFCA could not be detected within any of the reactor samples. After 10 h, FDCA selectivity reached 88.9 ± 1.9%, while DFF selectivity dropped to 9.0 ± 0.3%.

The remarkable catalytic activity of pulcherrimin, compared to Fe_2O_3/C, can be attributed to its unique metal–organic complex structure and the presence of nitrogen functional groups, as confirmed by FT-IR. These groups confer basicity, which facilitates oxidation reactions, a critical factor in enhancing the catalytic oxidation of 5-HMF. The Fe^{3+} sites within the pulcherrimin complex, identified through Mössbauer spectroscopy as high-spin Fe^{3+} species, facilitate direct electron transfer with the reactant molecules, thus actively participating in the oxidation process. Moreover, the mesoporous structure of pulcherrimin, as evidenced by BET surface area analysis and SEM images, enhances reactant accessibility to active sites, making pulcherrimin a highly effective catalyst for the oxidation of 5-HMF to FDCA, outperforming conventional Fe_2O_3/C systems. Compared to noble metal catalysts, pulcherrimin eliminates the need for precious metals and potential toxicity concerns. The base-free reaction avoids waste generation from neutralisation steps required in systems with homogeneous base co-catalysts.

To further evaluate the catalytic performance of pulcherrimin, the effect of temperature on the conversion of 5-HMF and the selectivity of its major oxidation products, DFF and FDCA, was examined at 100 °C, and 140 °C (Fig. 5). These temperatures were selected based on the thermal stability of pulcherrimin as discussed above. At 100 °C (Fig. 5a), after 10 h of reaction, 57.7 ± 0.5% of 5-HMF was converted, with a highly selective formation of DFF (99.0 ± 0.6%), indicating selective oxidation of the hydroxymethyl group (–CH_2OH) to an aldehyde group (–CHO). This observation aligns with literature reports suggesting that 5-HMF oxidation at lower temperatures primarily yields DFF.[48]

At 120 °C, the conversion of 5-HMF significantly increased to 73.3 ± 1.1%, accompanied by a dramatic shift in selectivity. DFF selectivity dropped to 9.0 ± 0.3%, while FDCA selectivity rose to 89.0 ± 1.9%. However, at 140 °C (Fig. 5c), while the conversion of 5-HMF increased slightly to 77.0 ± 0.8%, the selectivity for FDCA decreased to 57.2 ± 2.3%. The reduction in FDCA selectivity at elevated temperatures is attributed to its decomposition into side products, as indicated by the emergence of peaks corresponding to formic acid and levulinic acid. At the same time, the pH of the reaction solution decreased from 4.2 to 2.8 after 10 h reaction at 140 °C. These findings are consistent with reports that elevated temperatures can cause the furan ring to decompose into smaller molecules, particularly under acidic conditions.[49]

Effect of base addition. To evaluate whether the alkaline aqueous solution could further enhance the conversion of 5-HMF over pulcherrimin, 0.008 M NaOH was added to the reaction mixture. Since pulcherrimin is unstable under strongly alkaline conditions, a mild base was selected for this study. Consistent with the results over the Fe_2O_3/C catalyst, the addition of the base promoted the HMFCA route (Fig. 6). After 2 h of reaction, the primary product was HMFCA with a selectivity of 76.7 ± 0.9%, followed by DFF at 20.9 ± 0.8%, and a small amount of FDCA at 2.4 ± 0.3%. In contrast, in the non-base-added reaction, the primary product was 94.7 ± 0.5% DFF and 3.2 ± 0.1% FDCA.

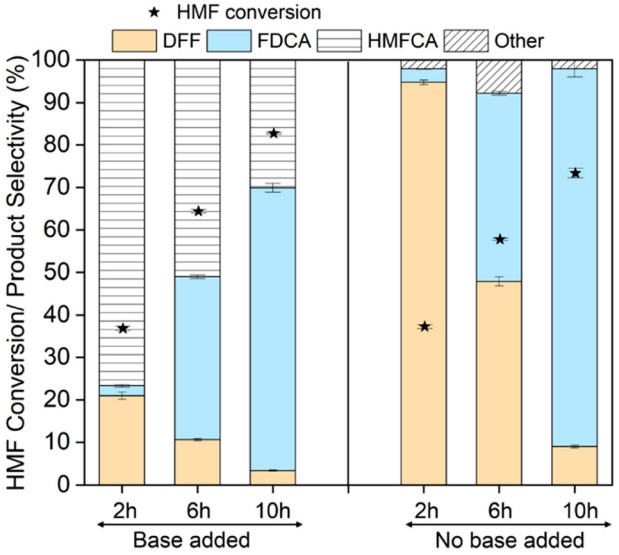

Fig. 6 Effect of addition of base: 5-HMF conversion and product selectivity with respect to time over pulcherrimin with and without the addition of a base (Reaction conditions: 40 mL of 4.15 mmol 5-HMF, 0.05 g of pulcherrimin, temperature 120 °C, 10 bar O_2 gas, for base added reaction: 0.008 M NaOH was added) (HMFCA was calculated by difference).

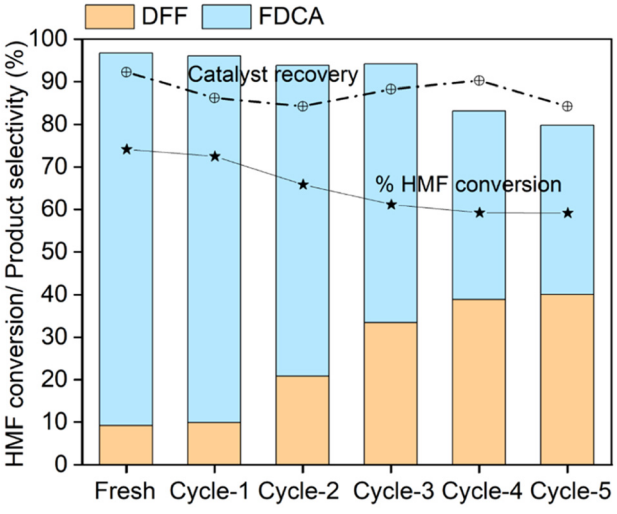

Fig. 7 Catalyst reusability studies: catalyst recovery, 5-HMF conversion and DFF and FDCA yields over pulcherrimin catalyst for 5 reaction cycles (Reaction conditions: 40 mL of 4.15 mmol 5-HMF, 0.05 g of pulcherrimin, temperature 120 °C, 10 bar O_2 gas, 10 h).

Throughout the reaction, the addition of the base increased the overall conversion of HMF; however, this came at the expense of FDCA selectivity, as the base primarily enhanced the formation of HMFCA rather than promoting further oxidation to FDCA. The final yields of FDCA in the base-added system were lower compared to the non-base-added reaction, indicating that the use of a base did not effectively enhance the production of the desired FDCA. At the end of 10 h, 82.5 ± 0.2% HMF was converted to DFF, FDCA, and HMFCA with selectivities of 3.4 ± 0.2%, 66.5 ± 1.05%, and 29.3 ± 0.2%, respectively.

Based on these findings, the addition of a base to the reaction system shifts the product distribution towards multiple intermediates, such as HMFCA and DFF, thus complicating the subsequent separation to isolate FDCA. Additionally, the presence of a base raises concerns about pulcherrimin stability. The product collected at the end of the reaction was mildly red, suggesting possible leaching of pulcherrimin, and the reactor vessel exhibited a mild red coating, potentially due to either corrosion or pulcherrimin leaching. Therefore, base addition did not prove to be advantageous in this case, as it complicates the reaction system, increases the difficulty of product separation, without significant enhancement of FDCA production.

3.2.3. Catalyst reusability tests. The reusability of pulcherrimin for the oxidation of 5-HMF was evaluated over five consecutive cycles, with the primary aim of assessing its stability under reaction conditions (Fig. 7). The primary focus of the study was to analyse the catalyst's stability by monitoring the conversion of 5-HMF and the selectivity for DFF and FDCA in each cycle. The catalyst recovery ranged from 84% to 92%, with most loss attributed to the catalyst adhering to the reactor vessel and head. To compensate for catalyst losses, fresh catalyst was added for repeatability studies. As discussed earlier, with fresh catalyst, 5-HMF conversion reached 73.3% after 10 h, with FDCA selectivity at 88.9% and DFF selectivity at 9.0%.

In subsequent cycles, a noticeable decrease in 5-HMF conversion was observed. By the second cycle, the conversion dropped to 65.8%; by the fifth cycle, it further reduced to approximately 59.1%. These losses in conversion are comparable to those reported in studies of other catalysts, particularly those operating under hydrothermal conditions, where metal leaching and structural degradation are common concerns.[50] Therefore, the observed degradation of pulcherrimin in an aqueous solvent highlights the susceptibility of such complexes to hydrolytic conditions. In contrast, Fe_2O_3-based catalysts exhibit more stable performance across cycles in organic solvents.[51]

The reaction rate for FDCA formation decreased significantly over time, with selectivity declining from 88.9% in the fresh cycle to 39.8% by the fifth cycle. This decline suggests that while the process favoured the DFF pathway for FDCA formation, other undetected by-products, such as non-volatile compounds or coke, may have formed, contributing to the loss in selectivity. Simultaneously, DFF selectivity increased from 9.0% in the fresh cycle to 40.0% in the fifth cycle. The shift in product selectivity further indicates that the catalyst's active sites, particularly those responsible for more profound oxidation to FDCA, are likely affected by prolonged exposure to aqueous conditions.

The catalyst recovered after five reaction cycles was analysed using ICP analysis to assess Fe leaching. The Fe content in

fresh pulcherrimin was 11.2 ± 0.2%, which decreased to 10.4 ± 0.3% after five cycles. This minor reduction suggests that Fe leaching is minimal and unlikely to fully account for the observed decline in catalytic activity. Other potential factors contributing to deactivation may include the loss of the metal–organic complex structure, which could reduce access to active sites or changes in the catalyst's basicity.

Future studies will focus on the detailed material characterisation of the spent catalyst to provide valuable insights into the catalyst deactivation mechanism and explore strategies to enhance catalyst stability and performance in subsequent applications. To improve stability in practical applications, techniques such as optimising catalyst recovery and reactivation and employing reactor configurations designed to minimise degradation should be explored. For example, methods such as heat treatment or washing to remove byproducts that may poison active sites could be evaluated. Modifying the reactor configuration to reduce catalyst exposure to extreme conditions or utilising flow reactors with continuous catalyst regeneration could reduce and minimise deactivation.[52] While this study highlights the potential for greener catalytic processes, a comprehensive sustainability assessment, including economic viability, LCA, and social impact, is necessary to fully substantiate these claims.[53]

3.3. Economic and environmental perspectives

A preliminary techno-economic analysis was conducted to compare the proposed pulcherrimin catalyst system with a conventional 5% Pt/C catalyst system,[54] evaluating key parameters such as catalyst cost, energy consumption, and FDCA purification and recovery processes and the values are given in Table 1.

3.3.1. Comparative insights

Cost efficiency. Our cost estimates confirm that pulcherrimin catalyst could be produced at a fraction of the cost as the baseline 5%Pt/C catalyst ($1.57 *vs.* $194 per kg). In addition, catalyst loading used in our study was ten times lower than used in the reference study. Despite this, estimated catalyst regeneration/replacement costs are approximately three times higher than for 5% Pt/C, due to the higher level of deactivation. While the reference study assumed the need for only 10% catalyst regeneration (at 20% of fresh catalyst cost) after 6 months of operation, we assumed 18.4% complete catalyst replacement after each 10 h reaction, in line with catalyst deactivation observed during our catalyst reusability studies. These findings demonstrate that only small improvements in pulcherrimin stability could significantly enhance the economic viability of the pulcherrimin system. This could be achieved by switching from the batch to a continuous system, as demonstrated previously for aqueous phase reforming reactions under similar conditions.[52] Moreover, we did not test the potential for catalyst reactivation to prolong catalyst lifetime (20% of new catalyst cost), iron recovery from spent catalyst (31% of total catalyst cost), or consider other by-products formed during pulcherrimin synthesis, which could help offset catalyst costs.

Energy costs for the pulcherrimin system are slightly higher ($0.153 *vs.* $0.087 per kg FDCA), but did not consider the impact of shorter reaction time (10 h *vs.* 16 h), use of milder reaction conditions and the use of water-only solvent, which would be expected to reduce these costs to a similar level as those for Pt/C. Both systems benefit from the lack of a base co-catalyst, significantly simplifying downstream separation and purification. Therefore, based on these preliminary non-optimised results, pulcherrimin promises to deliver similar economic performance to a state-of-the-art noble metal catalyst system.

Yield and conversion. The Pt/C catalyst achieves a higher FDCA yield (96.6%) compared to pulcherrimin (65.2% yield). Despite this, the economic advantages of pulcherrimin, particularly its significantly lower raw material cost, help offset its slightly lower performance. The trade-off between high catalyst regeneration costs and improved sustainability makes pulcherrimin a promising alternative for cost-conscious and environmentally friendly applications.

In addition to the techno-economic analysis, the environmental credentials of our Pulcherrimin system were compared to the state of the art Pt/C and Pd/C catalyst systems *via* E-factor analysis (Table 2). Calculations are focused on the 5-HMF oxidation reaction only, considering the amounts of reagent, solvent, base and catalyst consumed during each run. Solvent consumption is estimated at 10%, based on previously reported solvent recovery of 91.3% from a biphasic 5-HMF production system.[55] Estimated catalyst consumption are based on values calculated in economic analysis (1% for Pt/C and Pd/C, 18.4% for pulcherrimin), while substrate mass and product yield are obtained from respective studies.

The results indicate a slightly larger E-factor for pulcherrimin than for the two baseline systems, which can be explained by slightly lower activity and selectivity for the pulcherrimin system. In all cases, the E-factor is dominated by the use of solvent, while catalyst deactivation is minimal in all cases. As the solvent in our system is water, the associated environmental impacts are mainly associated with the energy losses of water evaporation, rather than creation of waste. However, these calculations do not consider the large material consumption during catalyst synthesis and regeneration, which can be

Table 1 Comparative techno-economic analysis of FDCA production using 5% Pt/C (reference catalyst) and pulcherrimin

Catalyst system	FDCA yield (%)	Catalyst loading (g g^{-1} HMF)	Catalyst cost ($ per kg)	Catalyst regeneration cost $ per kg FDCA	Energy cost $ per kg FDCA
5% Pt/C[54]	96.6	1.03 g	194	0.014	0.087
Pulcherrimin	65.2	0.1 g	1.57	0.045	0.153

Table 2 Comparison of *E*-factor values for different catalytic systems in FDCA production (per kg FDCA)[a]

Catalyst system	Reactant (kg kg^{-1})		Solvent (kg kg^{-1})		Catalyst (g kg^{-1})		Total inputs (kg kg^{-1})	Mass raw waste (kg kg^{-1})	Mass recovered waste (kg kg^{-1})	E-factor
	5-HMF	Base	Total	Recovery	Total	Recovery				
Pt/C	1.27	0.817	68.2	61.3	0.438	0.438	70.7	69.7	61.8	7.90
Pd/C	1.41	0.910	75.8	68.3	0.509	0.504	78.7	77.7	68.8	8.91
Pulcherrimin (this work)	1.53	0.00	118	106	0.147	0.118	119	118	106	12.4

[a] Check ESI† for detailed calculations.

orders of magnitude greater for the mining and refining of noble metals, than they are for the biological synthesis of pulcherrimin. Moreover, impacts of pulcherrimin synthesis could be partially offset by the production of other valuable metabolites, such as lipids,[56] while further optimisation to improve catalyst activity, stability and recovery could increase product yields and reduce the E-factor of the 5-HMF oxidation reaction. Therefore, pulcherrimin catalyst could deliver similar performance to the state-of-the art noble metal catalyst, but with significantly lower impacts when including wastes associated with catalyst synthesis and regeneration.

4. Conclusions

This study demonstrates the catalytic potential of pulcherrimin for the oxidation of 5-HMF to high-value products, particularly FDCA, under mild, base-free conditions. At 120 °C and 10 bar O_2 pressure, 73.3 ± 1.1% of 5-HMF was converted, selectively producing 88.9 ± 1.9% FDCA and 9.0 ± 0.3% DFF within 10 h without the need for any base. The addition of base altered the reaction mechanism, favouring the formation of HMFCA over DFF, highlighting the tunability of pulcherrimin's catalytic behaviour. Temperature also influenced the product distribution, with selective production of DFF at 100 °C, while 120 °C predominantly yielded FDCA.

Furthermore, the ability of pulcherrimin to selectively catalyse the oxidation of 5-HMF to FDCA, with moderate stability over multiple reaction cycles, highlights its potential as an effective catalyst for industrial applications. While the recycling of pulcherrimin shows some decline in activity after the second cycle, these findings underscore opportunities for optimisation, such as increasing the yield during pulcherrimin production *via* fermentation, adjusting reaction conditions, or improving reactor design to enhance both stability and catalytic performance. With additional research focused on fine-tuning its catalytic properties, pulcherrimin could be optimised for sustainable, large-scale applications, advancing green chemistry and contributing to a more sustainable chemical industry. This research positions pulcherrimin as a promising candidate for future biomass conversion processes, offering environmental and economic advantages by reducing reliance on harsh chemical conditions while efficiently producing value-added products like FDCA.

Data availability

The data supporting this article have been included as part of the ESI.†

Conflicts of interest

There are no conflicts to declare.

Acknowledgements

This work was supported by Biomass Biorefinery Network (BBNet), a BBSRC/EPSRC funded Network in Industrial Biotechnology and Bioenergy (BBSRC NIBB) BB/S009779/1 and UKRI-EPSRC through the Interdisciplinary Centre for Circular Chemical Economy (EP/V011863/1). The authors sincerely acknowledge the facilities and assistance provided by Loughborough Materials Characterisation Centre (LMCC) at Loughborough University.

References

1 M. J. Biddy, C. Scarlata and C. Kinchin, *Chemicals from biomass: a market assessment of bioproducts with near-term potential*, National Renewable Energy Lab. (NREL), Golden, CO, United States, 2016.
2 S. Mukundan, D. Boffito, A. Shrotri, L. Atanda, J. Beltramini and G. Patience, Thermocatalytic hydrodeoxygenation and depolymerization of waste lignin to oxygenates and biofuels in a continuous flow reactor at atmospheric pressure, *ACS Sustainable Chem. Eng.*, 2020, **8**(35), 13195–13205.
3 E. A. R. Zuiderveen, K. J. J. Kuipers, C. Caldeira, S. V. Hanssen, M. K. van der Hulst, M. M. J. de Jonge, *et al.*, The potential of emerging bio-based products to reduce environmental impacts, *Nat. Commun.*, 2023, **14**(1), 8521.
4 J. Sparks, C. Scaldaferri, A. Welfle, P. Thornley, A. Victoria and C. Donnison*et al.*, *Carbon for Chemicals: How can biomass contribute to the defossilisation of the chemicals sector?*, 2024.
5 A. Kumar, A. S. Chauhan, R. Bains and P. Das, Catalytic transformations for agro-waste conversion to 5-hydroxy-

methylfurfural and furfural: Chemistry and scale-up development, *Green Chem.*, 2023, **25**(3), 849–870.
6 S. Fulignati, D. Licursi, N. Di Fidio, C. Antonetti and A. M. Raspolli Galletti, Novel challenges on the catalytic synthesis of 5-hydroxymethylfurfural (HMF) from real feedstocks, *Catalysts*, 2022, **12**(12), 1664.
7 C. Xie, Z. Jiang, Y. Pang, C. Xiao and J. Song, Carbon-based catalytic materials for aerobic oxidative transformation of 5-hydroxymethylfurfural: advancements, challenges, and opportunities, *Green Chem.*, 2024, **26**, 6886–6899.
8 G. Totaro, L. Sisti, P. Marchese, M. Colonna, A. Romano, C. Gioia, *et al.*, Current Advances in the Sustainable Conversion of 5–Hydroxymethylfurfural into 2, 5–Furandicarboxylic Acid, *ChemSusChem*, 2022, **15**(13), e202200501.
9 A. Eerhart, A. P. C. Faaij and M. K. Patel, Replacing fossil based PET with biobased PEF; process analysis, energy and GHG balance, *Energy Environ. Sci.*, 2012, **5**(4), 6407–6422.
10 S. V. Suba, P. Sangavi, K. Nachammai and K. Langeswaran, Economics of Bioplastics and Biobased Products, in *Biodegradable Polymers, Blends and Biocomposites*, CRC Press, 2024, pp. 219–232.
11 J. G. Rosenboom, R. Langer and G. Traverso, Bioplastics for a circular economy, *Nat. Rev. Mater.*, 2022, **7**(2), 117–137.
12 J. Dai, Synthesis of 2,5-diformylfuran from renewable carbohydrates and its applications: A review, *Green Energy Environ.*, 2021, **6**(1), 22–32.
13 A. Al Ghatta, J. D. E. T. Wilton-Ely and J. P. Hallett, From sugars to FDCA: a techno-economic assessment using a design concept based on solvent selection and carbon dioxide emissions, *Green Chem.*, 2021, **23**(4), 1716–1733.
14 G. Trapasso, M. Annatelli, D. Dalla Torre and F. Aricò, Synthesis of 2,5-furandicarboxylic acid dimethyl ester from galactaric acid via dimethyl carbonate chemistry, *Green Chem.*, 2022, **24**(7), 2766–2771.
15 N. van Strien, S. Rautiainen, M. Asikainen, D. A. Thomas, J. Linnekoski, K. Niemelä, *et al.*, A unique pathway to platform chemicals: aldaric acids as stable intermediates for the synthesis of furandicarboxylic acid esters, *Green Chem.*, 2020, **22**(23), 8271–8277.
16 R. Mariscal, P. Maireles-Torres, M. Ojeda, I. Sádaba and M. L. Granados, Furfural: a renewable and versatile platform molecule for the synthesis of chemicals and fuels, *Energy Environ. Sci.*, 2016, **9**(4), 1144–1189.
17 S. Zhang, G. Chu, S. Wang, J. Ma and C. Wang, Base-Free Oxidation of HMF to FDCA over Ru/Cu-Co-O·MgO under Aqueous Conditions, *Molecules*, 2024, **29**(13), 3213.
18 R. J. van Putten, J. C. Van Der Waal, E. D. De Jong, C. B. Rasrendra, H. J. Heeres and J. G. de Vries, Hydroxymethylfurfural, a versatile platform chemical made from renewable resources, *Chem. Rev.*, 2013, **113**(3), 1499–1597.
19 D. Zhao, T. Su, Y. Wang, R. S. Varma and C. Len, Recent advances in catalytic oxidation of 5-hydroxymethylfurfural, *Mol. Catal.*, 2020, **495**, 111133.
20 F. Yang, J. Liu, B. Li, H. Li and Z. Jiang, Effective biosynthesis of 2, 5-furandicarboxylic acid from 5-hydroxymethylfurfural via a bi-enzymatic cascade system using bacterial laccase and fungal alcohol oxidase, *Biotechnol. Biofuels Bioprod.*, 2023, **16**(1), 164.
21 M. M. Cajnko, U. Novak, M. Grilc and B. Likozar, Enzymatic conversion reactions of 5-hydroxymethylfurfural (HMF) to bio-based 2, 5-diformylfuran (DFF) and 2, 5-furandicarboxylic acid (FDCA) with air: mechanisms, pathways and synthesis selectivity, *Biotechnol. Biofuels*, 2020, **13**, 1–11.
22 A. Serrano, E. Calviño, J. Carro, M. I. Sánchez-Ruiz, F. J. Cañada and A. T. Martínez, Complete oxidation of hydroxymethylfurfural to furandicarboxylic acid by aryl-alcohol oxidase, *Biotechnol. Biofuels*, 2019, **12**, 1–12.
23 G. Premaratne, R. Nerimetla, R. Matlock, L. Sunday, R. S. Hikkaduwa Koralege, J. D. Ramsey, *et al.*, Stability, scalability, and reusability of a volume efficient biocatalytic system constructed on magnetic nanoparticles, *Catal. Sci. Technol.*, 2016, **6**(7), 2361–2369.
24 A. J. Kluyver, J. P. Van Der Walt and A. J. Van Triet, Pulcherrimin, the pigment of Candida pulcherrima, *Proc. Natl. Acad. Sci. U. S. A.*, 1953, **39**(7), 583–593.
25 A. H. Cook and C. A. Slater, The structure of pulcherrimin, *J. Chem. Soc. (Resumed)*, 1956, 4133–4135.
26 E. Pawlikowska, B. Kolesińska, M. Nowacka and D. Kregiel, A new approach to producing high yields of pulcherrimin from Metschnikowia yeasts, *Fermentation*, 2020, **6**(4), 114.
27 F. Abeln, R. H. Hicks, H. Auta, M. Moreno-Beltrán, L. Longanesi, D. A. Henk, *et al.*, Semi-continuous pilot-scale microbial oil production with Metschnikowia pulcherrima on starch hydrolysate, *Biotechnol. Biofuels*, 2020, **13**, 1–12.
28 T. Chantasuban, F. Santomauro, D. Gore-Lloyd, S. Parsons, D. Henk, R. J. Scott, *et al.*, Elevated production of the aromatic fragrance molecule, 2–phenylethanol, using Metschnikowia pulcherrima through both de novo and ex novo conversion in batch and continuous modes, *J. Chem. Technol. Biotechnol.*, 2018, **93**(8), 2118–2130.
29 F. Abeln, R. H. Hicks, H. Auta, M. Moreno-Beltrán, L. Longanesi, D. A. Henk, *et al.*, Semi-continuous pilot-scale microbial oil production with Metschnikowia pulcherrima on starch hydrolysate, *Biotechnol. Biofuels*, 2020, **13**(1), 127.
30 S. Bettencourt, C. Miranda, T. A. Pozdniakova, P. Sampaio, R. Franco-Duarte and C. Pais, Single Cell Oil Production by Oleaginous Yeasts Grown in Synthetic and Waste-Derived Volatile Fatty Acids, *Microorganisms*, 2020, **8**(11), 1809.
31 H. Bejaoui, F. Mathieu, P. Taillandier and A. Lebrihi, Ochratoxin A removal in synthetic and natural grape juices by selected oenological Saccharomyces strains, *J. Appl. Microbiol.*, 2004, **97**, 1038.
32 S. Mukundan, J. Xuan, S. E. Dann and J. L. Wagner, Highly active and magnetically recoverable heterogeneous catalyst for hydrothermal liquefaction of biomass into high quality bio-oil, *Bioresour. Technol.*, 2023, **369**, 128479.
33 P. Randazzo, A. Aubert-Frambourg, A. Guillot and S. Auger, The MarR-like protein PchR (YvmB) regulates expression of genes involved in pulcherriminic acid biosynthesis and in the initiation of sporulation in Bacillus subtilis, *BMC Microbiol.*, 2016, **16**(1), 190.

34 E. A. Permyakov, The use of UV–vis absorption spectroscopy for studies of natively disordered proteins, *Intrinsically Disordered Protein Analysis: Volume 1, Methods and Experimental Tools*, 2012, pp. 421–433.
35 Y. Liu, Y. Li and K. S. Schanze, Photophysics of π-conjugated oligomers and polymers that contain transition metal complexes, *J. Photochem. Photobiol., C*, 2002, **3**(1), 1–23.
36 D. M. Kirschenbaum and F. S. Parker, The infra-red spectra of aqueous solutions of biogenic amine hydrochlorides, *Spectrochim. Acta*, 1961, **17**(8), 785–794.
37 F. Parker, *Applications of infrared spectroscopy in biochemistry, biology, and medicine*, Springer Science & Business Media, 2012.
38 J. Coates, Interpretation of infrared spectra, a practical approach, *Encyclopedia of analytical chemistry*, 2000, vol. 12, pp. 10815–10837.
39 M. Dawkins, D. Saal, J. F. Marco, J. Reynolds and S. Dann, An iron ore-based catalyst for producing hydrogen and metallurgical carbon via catalytic methane pyrolysis for decarbonisation of the steel industry, *Int. J. Hydrogen Energy*, 2023, **48**(57), 21765–21777.
40 J. C. MacDonald, Biosynthesis of pulcherriminic acid, *Biochem. J.*, 1965, **96**(2), 533.
41 A. Zdaniauskienė, T. Charkova, I. Ignatjev, V. Melvydas, R. Garjonytė, I. Matulaitienė, *et al.*, Shell-isolated nanoparticle-enhanced Raman spectroscopy for characterization of living yeast cells, *Spectrochim. Acta, Part A*, 2020, **240**, 118560.
42 K. Mažeika, L. Šiliauskas, G. Skridlaitė, A. Matelis, R. Garjonytė, A. Paškevičius, *et al.*, Features of iron accumulation at high concentration in pulcherrimin-producing Metschnikowia yeast biomass, *JBIC, J. Biol. Inorg. Chem.*, 2021, **26**, 299–311.
43 R. Jaiswal and K. V. S. Ranganath, Carbon nanoparticles on magnetite: a new heterogeneous catalyst for the oxidation of 5-hydroxymethylfurfural (5-HMF) to 2, 5-diformoylfuran (DFF), *J. Inorg. Organomet. Polym. Mater.*, 2021, **31**(12), 4504–4511.
44 R. Fang, R. Luque and Y. Li, Selective aerobic oxidation of biomass-derived HMF to 2, 5-diformylfuran using a MOF-derived magnetic hollow Fe–Co nanocatalyst, *Green Chem.*, 2016, **18**(10), 3152–3157.
45 G. Totaro, L. Sisti, P. Marchese, M. Colonna, A. Romano, C. Gioia, *et al.*, Current Advances in the Sustainable Conversion of 5−Hydroxymethylfurfural into 2, 5−Furandicarboxylic Acid, *ChemSusChem*, 2022, **15**(13), e202200501.
46 T. W. Chamberlain, V. Degirmenci and R. I. Walton, Oxidation of 5−Hydroxymethyl Furfural to 2, 5−Furan Dicarboxylic Acid Under Mild Aqueous Conditions Catalysed by MIL–100 (Fe) Metal–Organic Framework, *ChemCatChem*, 2022, **14**(7), e202200135.
47 O. R. Schade, K. F. Kalz, D. Neukum, W. Kleist and J. D. Grunwaldt, Supported gold-and silver-based catalysts for the selective aerobic oxidation of 5-(hydroxymethyl) furfural to 2, 5-furandicarboxylic acid and 5-hydroxymethyl-2-furancarboxylic acid, *Green Chem.*, 2018, **20**(15), 3530–3541.
48 H. Liu, X. Cao, J. Wei, W. Jia, M. Li, X. Tang, *et al.*, Efficient aerobic oxidation of 5-hydroxymethylfurfural to 2, 5-diformylfuran over Fe2O3-promoted MnO_2 catalyst, *ACS Sustainable Chem. Eng.*, 2019, **7**(8), 7812–7822.
49 K. Tashiro, M. Kobayashi, K. Nakajima and T. Taketsugu, Computational survey of humin formation from 5-(hydroxymethyl) furfural under basic conditions, *RSC Adv.*, 2023, **13**(24), 16293–16299.
50 J. Huo, J. P. Tessonnier and B. H. Shanks, Improving Hydrothermal Stability of Supported Metal Catalysts for Biomass Conversions: A Review, *ACS Catal.*, 2021, **11**(9), 5248–5270.
51 X. Liu, H. Xu, X. Fu and J. Chen, Steam-Assisted Synthesis of Hectorite Loaded with Fe2O3 and Its Catalytic Fenton Degradation of Phenol, *Catalysts*, 2024, **14**(8), 521.
52 P. Nagy, D. R. Inns, S. A. Kondrat and J. L. Wagner, The effect of flow conditions on the activity and stability of Pt/LaAlO3 perovskite catalyst during aqueous phase reforming of glycerol, *Chem. Eng. J.*, 2024, **483**, 149274.
53 A. Bardow, J. Pérez-Ramírez, S. Sala and L. Vaccaro, Measuring green chemistry: methods, models, and metrics, *Green Chem.*, 2024, **26**(22), 11016–11018.
54 A. Hussain Motagamwala, W. Won, C. Sener, D. M. Alonso, C. T. Maravelias and J. A. Dumesic, Toward biomass-derived renewable plastics: Production of 2,5-furandicarboxylic acid from fructose, *Sci. Adv.*, 2018, **4**, eaap9722.
55 M. Sayed, N. Warlin, C. Hulteberg, I. Munslow, S. Lundmark, O. Pajalic, *et al.*, 5-Hydroxymethylfurfural from fructose: An efficient continuous process in a water-dimethyl carbonate biphasic system with high yield product recovery, *Green Chem.*, 2020, **22**(16), 5402–5413.
56 A. Němcová, M. Szotkowski, O. Samek, L. Cagáňová, M. Sipiczki and I. Márová, Use of waste substrates for the lipid production by yeasts of the genus metschnikowia—screening study, *Microorganisms*, 2021, **9**(11), 2295.